OPEN ACCESS

University of Dundee

University of Dundee

Behaviour of saturated fibre-reinforced sand in centrifuge model tests

Wang, Ke; Brennan, Andrew

Published in:
Soil Dynamics and Earthquake Engineering

DOI:
10.1016/j.soildyn.2019.105749

Publication date:
2019

Licence:
CC BY-NC-ND

Document Version
Peer reviewed version

Link to publication in Discovery Research Portal

Citation for published version (APA):
Wang, K., & Brennan, A. (2019). Behaviour of saturated fibre-reinforced sand in centrifuge model tests. *Soil Dynamics and Earthquake Engineering*, *125*, 1-11. [105749]. https://doi.org/10.1016/j.soildyn.2019.105749

General rights
Copyright and moral rights for the publications made accessible in Discovery Research Portal are retained by the authors and/or other copyright owners and it is a condition of accessing publications that users recognise and abide by the legal requirements associated with these rights.

• Users may download and print one copy of any publication from Discovery Research Portal for the purpose of private study or research.
• You may not further distribute the material or use it for any profit-making activity or commercial gain.
• You may freely distribute the URL identifying the publication in the public portal.

Take down policy
If you believe that this document breaches copyright please contact us providing details, and we will remove access to the work immediately and investigate your claim.

Download date: 05. May. 2023

Title

Behaviour of Saturated Fibre-Reinforced Sand in Centrifuge Model Tests

Author names and affiliations

Ke Wang[1], Andrew Brennan[2]

[1] Changjiang River Scientific Research Institute of Changjiang Water Resources Commission, Wuhan, China (Formerly University of Dundee, Dundee, UK)

[2] University of Dundee, Dundee, UK

Corresponding author

Ke Wang

tonykewang@hotmail.com

Changjiang River Scientific Research Institute of Changjiang Water Resources Commission, Wuhan, 430010, China (Formerly University of Dundee, Dundee, DD1 4HN, UK)

© 2019. This manuscript version is made available under the CC-BY-NC-ND 4.0 license http://creativecommons.org/licenses/by-nc-nd/4.0/

Abstract

Fibre-reinforcement has shown its efficacy in improving soil properties and been proposed to apply in increasing liquefaction resistance of deposits. As the contributions of fibres in real seismic conditions are yet to clarify, further investigations are needed to fill this gap. In this study, centrifuge tests have been conducted for this exploration. The dry pluviation preparation procedures for fibre-reinforced sand in centrifuge testing are disclosed in details for the first time. Results show that fibres are beneficial in preventing structure collapse of the sand matrix, but liquefaction induced excess pore pressures and ground surface settlements reduction is not apparently reduced as those in previous tests. Shear moduli are enhanced to some extent under lower confining stresses at relative larger shear strain levels, while equivalent damping ratios are increased at small strain levels. Limitation of simulating real conditions of previous element tests and 1g shaking table tests may exaggerate the benefits of fibres.

Keywords

Fibre-reinforced sand
Liquefaction
Centrifuge modelling
Acceleration propagation
Excess pore pressure
Settlement
Shear modulus
Equivalent damping

1. Introduction

Earthquake-induced liquefaction has aroused considerable attention since the 1964 Niigata earthquake at which serious damage was caused by this phenomenon unexpectedly [1]. Numerous efforts have been made to clarify the basic mechanism and evaluate the susceptibility of soils to liquefaction. When a given site is susceptible to liquefaction, mitigation methods should be taken to reduce such risk. The conventional techniques adopted nowadays include replacement, densification, drainage, dewatering, grouting and mixing, shear strain limitation [2]. Considering the reliability, economic and environmental aspects, fibre-reinforcement as a new soil improvement technique has attracted increasing attention in geotechnical engineering in recent 30 years.

Extensive experiments have been conducted to investigate the benefits of fibres on sand properties under monotonic loadings. Direct shear tests [3, 4] and triaxial compression tests [5-9] have shown the capability of fibres in improving soils' peak strength and limiting their post-peak shear resistance losses. These benefits are mainly dependent on the cohesion of soil, grain sizes of soil, lengths and diameters of fibres, materials of fibres, fibre concentrations aspect ratios (length/diameter) of fibres, confining stresses and shear strains. Undrained triaxial tests and ring shear tests [10, 11] demonstrated the capability of fibres in reducing static liquefaction potential of saturated loose sand. Fibre-reinforced samples even maintained their own structures after removal of the membrane while corresponding unreinforced samples totally collapsed. This implies that the presence of fibres seems to impart additional strength to the soil under low confining stresses and has the potential to prevent the occurrence of lateral spreading in unreinforced cases.

Studies on the dynamic behaviour of fibre-reinforced soil are very limited in the literature. Based on the resonant column and torsional tests, Maher and Woods [12] found that the shear modulus of sand is increased by adding fibres and the effects become more pronounced under high shear strains and low confining stresses. However, the damping ratio is much less and even negligible at large strains level. Li and Senetakis [13] examined the effects of fibres on the dynamic responses of well-graded and uniform sand at small to medium strains by high-amplitude resonant column tests. At small strains, the shear moduli of both types of sand were reduced with the presence of fibres. At medium strains, fibres increased the shear modulus of well-graded sand but not apparently affected that of the uniform sand. Moreover, the damping ratios at

medium strains were increased in both types of sand by fibres. The contribution of fibre-reinforcement to dry backfill behind sheet pile retaining wall was investigated by Jamshidi and his colleagues [14] through 1g shaking table tests. They also found that the shear modulus of fibre-reinforced sand is increased more at larger shear strains.

Effects of fibres on improving liquefaction resistance were initially studied by Noorany and Uzdavines [15] using undrained cyclic triaxial tests. It was showed that specimens reinforced by randomly distributed fibres have higher liquefaction resistance than other reinforcement types. Similar tests conducted by other researchers also showed benefits of polypropylene fibres [16] and coir fibres [17] on improving liquefaction resistance of the sand. Besides sand, liquefaction potential of the fly ash is also significantly reduced and it is even arrested by the presence fibres and it is more pronounced at low confining stresses [18].

In the 1g shaking table tests conducted by Maheshwari et al. [19], synthetic fibres reduced up to 90% of the excess pore pressure and 80% of the ground settlement, and prolonged the excess pore pressure build-up time by 50% in the saturated sand under 0.1g sinusoidal excitation, implying encouraging potential of using fibre-reinforcement against liquefaction in free field at depths of up to 0.6m.

Although effects of fibres on the dynamic responses of saturated sand have been shown in laboratory tests mentioned above, the efficacy of the real improvement can be better replicated for investigation under real stress strain conditions which are encountered in the field. In order to replicate such real stress strain conditions in small scaled physical models, geotechnical centrifuge modelling is needed for further studies. This work aims to obtain the contribution of fibres to the dynamic responses and liquefaction resistance of sand in real free field conditions. Preparation procedures of saturated fibre-reinforced sand for centrifuge testing are described in details and effects of fibres on acceleration propagation, excess pore pressure generation and ground settlement are evaluated from comparisons between two centrifuge tests. One test is for the benchmark scenario in which liquefiable soil is unreinforced and the other is for the extreme reinforcement scenario in which the entire liquefiable soil is fibre-reinforced, devised to show the maximum possible benefit from the technique. Influences on shear modulus and damping caused by the presence of fibres at various depths at the beginning of excitation are explored from the acceleration measurements in the deposit. The potential benefit of fibres as a ground improvement technique is also evaluated.

2. Centrifuge modelling

2.1. Equipment

In order to investigate the influence of fibre reinforced soils within a geotechnical system, a pair of centrifuge experiments were performed. The centrifuge tests were conducted under 50g (50 times earth gravity) on the Actidyn C67-2 geotechnical centrifuge with a nominal radius of 2.75m at the University of Dundee, and the earthquake was excited by the Actidyn Q67-2 servo-hydraulic one-dimensional earthquake simulator. More details about these facilities can be found in the work of Brennan et al. [20]. Models were constructed in an equivalent shear beam (ESB) container with internal dimensions of $674 \times 280 \times 312 mm^3$. This box consists of a rigid base plate and 6 stacked hollow rectangular rings which are sandwiched by rubber interfaces. This allows the lateral deformation of the box to match that of designed dry sand deposit. If the properties of the contained soil are largely different from those for which the ESB container designed, the side walls of the ESB container will interact evidently with the boundaries of the contained soil model [21]. The stiffness of saturated sand is highly nonlinear because it varies with effective stresses. Therefore, there are interactions between the ESB container and boundaries of the model consisting of saturated sand. However, it has been shown that such interactions are negligible within the central 300mm area of the model [22]. Three types of instruments were used to collect data during and after the earthquake. In this study, ADXL78 MEMS accelerometers (ACCs), 3-bar Druck PDCR81 pore pressure transducers (PPTs) and RDP LDC1000A linear variable differential transformers (LVDTs) were used for measuring accelerations, pore pressures and displacements respectively. More details about the equipment and instruments are described in the work of Bertalot [23].

2.2. Materials

HST 95 Congleton sand was used for deposit construction and flexible polypropylene crimped fibres with a commercial name Loksand^{TM} (Fig. 1) were used as the reinforcement material. The properties of sand and fibres are shown in Table 1 and Table 2. Neither the sand nor the Loksand^{TM} fibres are reduced in scale in the centrifuge tests. This is because the most important aspect of the test is achieving the same constitutive behaviour as the sand and sand-fibre composite in prototype, and the

most reliable way of achieving this is to use identical materials. Methylcellulose solution with a viscosity of 50 mPa·s was used as the pore fluid to ensure the time scales of dynamic effects and dissipation are matched [24]. A further discussion of centrifuge scaling laws can be found in the work of Muir Wood [25].

2.3. Model preparation

The general deposit layout and instrument distribution are shown in Fig. 2. The upper layer was constructed by loose sand with D_r=40%, representing a 10m liquefiable deposit, and the lower layer was built by dense sand with D_r=80% as a 4m non-liquefiable layer. The main ACCs and PPTs were installed in vertical arrays in the middle of the model to avoid the disturbance of boundary effects, and LVDTs were installed to measure the ground surface settlement of the central area in the models. When the sand deposit was constructed to a prescribed elevation, corresponding ACCs and PPTs were placed on the surface of the deposit. These sensors were then covered by the sand which was used for constructing the upper layer. These procedures were repeated until the completion of the deposit construction. The housing tubes of LVDTs were then fixed on a rigid frame across the ESB container, and the extension rods attached with plastic discs were extended to the surface of the deposit.

The model preparation procedures are schematically described in Fig. 3. The dense layer was constructed by pluviating sand by a slot pluviator at a controlled rate. As the slot pluviator was unable to construct a loose deposit adequately, the upper layer without fibres was built by a spot pluviator with circular opening 5mm mesh at the outlet. The uniformity of the deposits prepared by both types pluviators were checked by using small containers placed at various locations within the ESB container [26]. Variations in the relative density of sand prepared by slot and spot pluviators are within ±5% and ±7% respectively [27], indicating that reasonably uniform sand deposits can be prepared by both types of pluviators.

For the fibre-reinforced layer, the concentration of fibres, w_f, is defined as the dry weight of fibres (W_f) relative to the dry weight of the sand (W_s) [28]:

$$w_f = \frac{W_f}{W_s} \tag{1}$$

Dry pluviation was also used in building dry fibre-reinforced layer because the alternative method, moist tamping, is not compatible with the viscous pore fluid

required in this study as the composite prepared by the viscous fluid becomes hard once water is evaporated. If using water during mixing, the water content after construction is unknown resulting in an unpredictable viscosity of pore fluid.

The fibre-reinforced layer was subdivided into five equal layers (4 cm each in model scale) for construction to minimise the non-uniformity of the composite during preparation. From the bottom one-fifth sub-layer, fibres were manually put on the dense layer like a 'quilt'. Fibres should be randomly spread and not be concentrated or balled up in the 'quilt'. The average thickness of the quilt was around 5 cm for obtaining the desired layer thickness after pluviation as the falling sand particles squeeze the 'quilt' by their impact force. The uniformity of fibre distribution was visually monitored. Then the sand was pluviated by the slot pluviator. When sand deposit nearly reached the prescribed elevation, another 'quilt' was put on and combined with the beneath fibre layer manually to avoid the weak combination zone between sub-layers. These procedures were repeated until the whole deposit was constructed.

In the dry pluviation technique, the attained relative density of the sand is controlled by the pouring rate, particle impact velocity and the particle size [29]. To avoid the over squeeze and destruction of the fibre 'quilt', a small amount of sand with highest falling speed was adopted for attaining the largest fibre concentration at certain relative density. The slot pluviator was adjusted to the smallest opening (1mm) and increased to a height of 1.8m at which sand particles would have enough potential energy to achieve the terminal velocity before impact. All these conditions also meet with those for building the dense layer. The final impact velocity of sand particles is reduced by the buffer effect of the fibre quilt, resulting in a reduction of deposit relative density. As buffer effect is a function of the content of fibres, impact velocities of the particles (also the relative density of sand deposit) are closely related to the prescribed fibre concentrations. As the relative density of loose deposit constituted by clean sand was 40%, 0.6% in fibre concentration was adopted for keeping the same bulk density of the sand solid [30]. This fibre concentration is also reasonable for fibre-reinforcement because concentrations less than 1% were usually used in previous investigations [11, 16, 19] and the same concentration was also used in the previous works of other researchers using Loksand^{TM} as the reinforcement material [10, 28].

There is no uniform definition of the relative density of fibre-reinforced soil since the volume occupied by fibres can belong either to the solid sand particles or the voids [28]. In this study, fibres are considered as the part of voids. In other words, the fibres

take the space of voids, and the amount of sand between clean sand and fibre-reinforced sand are the same.

After dry pluviation, the methylcellulose solution, prepared in advance, was injected from the bottom at a very low rate to avoid the disturbance from seepage and drive the trapped void air out. The saturation process required at least 36 hours and the table of fluid was about 2mm above the deposit surface to guarantee the full saturation.

3. Test programme

All the tests were conducted at a nominal 50g level. This g level was achieved at a depth of 130mm (model scale) from the ground surface of models and the variation of g level in models was within ±6%. The input motion was a scaled record of the fault normal component from the Izmit station (NGA1165) in the Kocaeli earthquake, Turkey, 1999. The characteristics of the motion are shown in Fig. 4. The motion is required to be capable of liquefying soil but not to be unrealistically severe. This M_w 7.5 earthquake was selected to correspond with the "benchmark" magnitude used for liquefaction potential evaluation, e.g. the simplified procedure of Seed et al. [31]. The particular motion was taken as representative of rock accelerations in the vicinity of soil that was known to have been liquefied, thus providing a motion that is capable of liquefying soil but not excessively damaging. All the units in the direct results and analyses are in prototype unless specified.

4. Test results

4.1. Accelerations

Fig. 5 shows the acceleration time histories measured by the vertical ACC array in the middle of models. Acceleration amplitudes were amplified in the dense layer and then attenuated in the loose and fibre-reinforced layers. Accelerations started to attenuate significantly once they propagated to the bottom of the loose layer at the depth of 9m in the clean sand but not that apparently in the fibre-reinforced deposit until reaching the depth of 7m. As to the time aspect in the clean sand, acceleration amplitudes attenuated greatly after the strongest cycle at around 15s when excess pore pressures were high enough to significantly soften the soil at depths from 9m to 5m (Fig. 6), indicating that the soil deposit started to liquefy as expected. Similar attenuation also happened in the fibre-reinforced sand, but to a less extent (comparing

acceleration time histories in Fig. 5). It suggests that fibres in deposit improve propagation of accelerations at various vertical effective confining stresses, which implies some minor success in reducing stiffness loss and structure collapse of liquefied sand.

4.2. Excess pore pressures and ground settlements

The time histories of excess pore pressures generated during the earthquake and their dissipation after the earthquake at various depths are shown in Fig. 6. Both tests are plotted on the same axes in this figure, together with a horizontal dashed line indicating the initial vertical effective stress (labelled as "r_u=1") at which excess pore pressure is sufficient to support the full total stress applied (i.e. occurrence of liquefaction). The parameter r_u is the ratio of the excess pore pressure to the initial vertical effective stress. The time histories of excess pore pressures shown at a depth of 12m (within the dense deposit) in the fibre-reinforced model were not significantly lower than those in the benchmark (clean sand) model, implying that fibres may not apparently affect the excess pore pressures in the underneath deposit. The maximum values of excess pore pressures and the dissipation process were also not significantly different in both models, suggesting that fibres may not significantly affect these two aspects as well. During the generation process (from around 10s to 16s), the excess pore pressure rising rates at depths of 5m and 9m in the fibre-reinforced sand were slightly slower than those in clean sand. This suggests that the presence of fibres may reduce the rate of destruction of the sand matrix structure, which induces excess pore pressure. At the depth of 1m, transient excess pore pressure cycles with spikes were observed in the fibre reinforced sand, implying that fibre-reinforcement may even cause some dilation when the confining stress is low enough and shear strain is large enough. As such spikes are not seen in the clean sand, the dilation may be caused by relative movements between grains and fibres.

Fig. 7 depicts that there was no apparent difference in the ground surface settlements between the two deposits. This implies that the presence of fibres is not so beneficial to reduce the final volumetric strain in the liquefiable free field.

These are slight effects compared to the more marked reductions in excess pore pressure generation and apparent changes in volumetric strains (ground settlement) observed in element tests [32] and 1g shaking table tests [19]. It may, therefore, the

case that when the reinforced soil is loaded "naturally" rather than by imposed rams as in an element test, there may be insufficient strains to mobilise any benefit from fibres. In other words, the fibres may require large shear strains in order to have an effect. Element tests can provide these with constant loading amplitudes during soil softening caused by excess pore pressure, but the 'free field' examined here may not. To investigate this further, the stress-strain behaviour of the models is investigated.

5. Stress-strain behaviour

As models underwent one-dimensional shaking loads, the soil column within models can be idealised as a one dimensional shear beam. Calculation of the shear stress and shear strain through measurements of stacked accelerometers in this study is based on the work of Zeghal et al. [33] and Brennan et al. [34]. The method is valid for quarter-wavelengths longer than the separation distance between instruments. For a frequency range from 0.8Hz to 6 Hz and instrument spacing of 2m, this translates as being valid when soil shear wave velocity $V_s > 48$ m/s and might be valid when 6.4 m/s $< V_s < 48$ m/s. In other words, the derived stress strain loops may not be valid in some cases when the soil is softened by the increased excess pore pressure. This will be stated later in selecting representative loops. Acceleration data recorded by accelerometers are band-filtered before calculating stresses and strains. The lower limit and higher limit for the band-filtering are 0.8Hz and 6Hz respectively, which correspond to the boundary of the valid input motion frequency range (see Fig.4b). For the calculation of stresses and strains at specific depths, the first order approximation is used for shear stresses and the second order approximation is used for shear strains.

5.1. Shear stress--strain relationships

The relationship between shear stresses (τ) and shear strains (γ), which would be expected to show a hysteresis loop, can be derived from their time histories. A typical hysteresis loop for evaluating soil properties should incline to the first and third quadrant and the trace should rotate in a clockwise direction with time, which is schematically shown in Fig. 8. Using the method mentioned above requires the separation of accelerometers to be less than quarter-wavelength of vibration. It was found that the most hysteresis loops rarely fulfil the selection principles after 14.5s when the excess pore pressure increased to a certain level. This is caused by the fact

that the wavelength in the deposit during excitation became much shorter when the deposit was softened by the increase of excess pore pressure. Liquefied soil acted as a low pass filter. The fixed distance between adjacent accelerometers became larger than the quarter-wavelength, and "spatial aliasing" occurred. The stress--strain relationship calculated from the previous algorithm is not reliable at that time. Therefore, some representative loops during 9~14.5s are shown in Fig. 9 and used for the calculation in the next section. Specifically, for the clean sand case, six loops are selected from section 9~10.5s, nine loops from section 10.5~12s and six loops from section 12~14.5s. Correspondingly, for the fibre-reinforced sand case, six loops are selected from section 9~10.5s, ten loops from the section 10.5~12s and seven loops from section 12~14.5s. It should be acknowledged that some traces still may not be valid for representing the stress-strain relationships of the soil because of the complexity of the loading conditions and excess pore pressure generation.

The shear stress-strain loops at representative depths (1m, 3m, 5m and 7m) are divided into three periods (Fig. 9). The first period, from 9~10.5s, corresponds to small excitations before the excess pore pressure is generated. During the second period (10.5~12s), strong excitation with little excess pore pressures are observed. In the third period (12~14.5s), excitations are reduced with the obvious generation of excess pore pressures (see Fig. 5 and Fig. 6). The blue dashed curves and red dashed lines shown during the period 10.5~12s in Fig. 9 will be described in Section 5.2.

The difference between the clean sand and fibre-reinforced sand is not obvious during the first period (9.0~10.5s) as excitations appear to have been too gentle to induce significant strains within the soil. When the seismic loadings become larger during the second period (10.5~12.0s), the fibre reinforced sand shows some stiffening at depths of 1m and 3m when the shear strain level reaches 0.5% or more because of its steeper curves in shown Fig. 9. The behaviour at depths of 5m and 7m in both models are similar, but the loops of fibre-reinforced sand are fatter, implying that fibres are dissipating some energy (i.e. increasing the apparent damping). In the third period (12.0~14.5s), the both stress and strain levels in clean sand reduced dramatically, indicating a "self-limiting" phenomenon induced by the softening. The fibre reinforced sand still maintained the stress and strain levels to some extent, which corresponds with the earlier conclusions that the fibres were helping propagating accelerations.

5.2 Evaluation of shear moduli

As the input motion of this study has a variety of peak acceleration amplitudes and a broad banded frequency content, the shear hysteresis loops in this study are rarely nice clean ellipses like those obtained from element tests or centrifuge tests with sinusoidal input motions The representative stress-strain loops, which generally have the shape shown in Fig. 8, were manually selected from Fig. 9 (examples of representative loops are traced by blue dashed curves).

A relative robust way to obtain a representative equivalent shear modulus from an irregular loop is evaluating the ratio of the difference between the maximum shear stress and the minimum shear stress to the maximum shear strain (Brennan et al. 2005) shown in Fig. 8:

$$G = \frac{\Delta\tau}{\Delta\gamma} \tag{2}$$

$\Delta\tau$ is half of the total stress range and $\Delta\gamma$ is half of the total strain range.

The representative slopes for the traced loops, which mentioned earlier, are shown by the red dashed lines in Fig.9.

To compare calculated moduli and damping ratios with those derived from empirical equations, the maximum shear modulus (G_{max}) at very small shear strain, which is the key parameter, should be obtained first. G_{max} of both materials at various effective vertical confining stress (Fig.10) were obtained by bender element tests carried out by the variable direction dynamic cyclic simple shear (VDDCSS) system at the University of Dundee [35].

In this study, the dynamic behaviour of the deposit at depths of 1m, 3m, 5m and 7m were chosen as representative points for analysis. The values of r_u at depths of 1m and 5m were obtained directly from the measurement of PPTs. At depths of 3m and 7m, the values were obtained from the linear interpolation of measurement of the adjacent PPTs. The r_u values from the 9.0~11.5s period are very close to 0, so the shear moduli calculated from measurements during this period were used to select the modification parameters (a, b) in Eqs. (3) for the characteristic curves of shear moduli [36]. To maintain the hyperbolic shape and fit corresponding data points based on the least square method, a=-0.0387, b=0 were selected for the fibre reinforced sand and, a=0.7720, b=0 were for the clean sand.

$$\frac{G}{G_{\max}} = \frac{1}{1+\gamma_h} \tag{3a}$$

$$\gamma_h = \frac{\gamma}{\gamma_r}[1 + a \cdot \exp^{b(\frac{\gamma}{\gamma_r})}] \tag{3b}$$

$$\gamma_r = \frac{\tau_{\max}}{G_{\max}} \tag{3c}$$

where τ_{max} is the maximum shear stress.

5.3 Effects of fibres on shear moduli

The comparisons of shear moduli between the clean sand and the fibre-reinforced sand under various depths are shown in Fig. 11(a). The line between data points indicates the path of those changing shear moduli with shear strains. The solid bold curves represent the empirical shear modulus-strain relationship when r_u is the lowest and the dashed bold curves represent the relationships when r_u is the highest during the period of 0~14.5s.

Both models demonstrate a degradation trend of shear moduli and these trends match well with the solid curves when shear strains start to increase at the beginning of the excitation. Shear strains then become less because of the occurrence of "self-limiting" of softened soil induced by excess pore pressures. The data points return along the dashed curves rather than the original solid ones, implying dependence of the shear modulus on excess pore pressure variations. At shallower depths (1m, 3m and 5m), the shear moduli of the fibre reinforced sand are apparently larger than those of the clean sand when the models start to be sheared and excess pore pressures are negligible. At greater depth (7m) the shear moduli are quite similar in both models.

The centrifuge data points from both models cannot be compared with each other directly because it is impossible to find corresponding data points in the fibre-reinforced model having the same shear strains and excess pore pressures as those in the clean sand model. This is mainly due to the complexity of the input motion and different responses between the models. Although the empirical curves obtained earlier have limitations on precisely predicting the shear moduli of the sand, they reasonably described shear moduli changes caused by shear strains and excess pore pressures. For further clarification, the estimated shear moduli from selected representative loops are compared with those predicted by the empirical hyperbolic curves in Fig. 12. It shows

that the data points from fibre-reinforced sand and clean sand closely scatter around the perfectly matched line. This indicates that shear moduli derived from the empirical curves can be used for analysing the effects of fibres on soil's shear moduli. Therefore, the insight into the effects of fibres on shear modulus can be obtained by comparing the empirical curves. As shown in Fig. 13, the shear modulus ratios between the fibre-reinforced sand and the clean sand increase with the shear strains and the values at a certain shear strain decreases with the increase of effective vertical confining stress. These are in line with previous research conclusions [12, 14] and support the earlier conclusions that a certain level of shear strain is required to mobilise the maximum influence of the fibres. It also implies that fibres may be more effective with the rise of excess pore pressures (the reduction of effective confining stresses) to maintain the stiffness of soil at small strains.

5.4 Evaluation of damping ratios

The equivalent damping ratio (D) is calculated conventionally (Fig. 8): The energy dissipation (ΔW) is evaluated by estimating the area inside the representative loop bounds from a simple trapezoidal integration between data points [34].

$$D = \frac{1}{4\pi}\frac{\Delta W}{\Delta W_{elastic}} = \frac{1}{2\pi}\frac{\oint \tau d\gamma}{\Delta\tau \cdot \Delta\gamma} \tag{4a}$$

The maximum damping ratio ($D_{\max}$) is estimated to be 33.3%, which is a representative value for sand from previous researchers [36-38], and the empirical equation for the relationship between D and γ is also originated from the work of Hardin and Drnevich [36]:

$$D = \frac{\gamma_h}{1+\gamma_h} D_{\max} \tag{4b}$$

5.5 Effects of fibres on damping ratios

Except those at the depth of 1m, the damping ratios show a generally increasing trend with strains as expected (Fig. 11(b)). The decreasing trend at the depth of 1m is caused by the fact that the hysteresis loops are flattened when the shear strain increases to a certain level at a very low confining stress and the area of the loop (ΔW) decreases

dramatically. Although $W_{elastic}$ is also decreased, the amount is much less than that of ΔW. Similar results can also be found in the work of Talaganov [39].

The curves given by the empirical equations show a reasonable agreement with data points, but more broadly scattered compared with those in shear moduli. This may be due to the irregular shapes of the loops, inducing larger errors in the estimates of equivalent damping ratios. Such more broadly scattered data in damping ratios have also been observed by other researchers [34, 40, 41].

The damping ratios of the fibre-reinforced sand are larger than those of the clean sand at small strain (<0.5%) when excess pore pressures are small. The damping ratios in both types of sand become similar when shear strains become large enough together with greater excess pore pressures. The limitation of comparison through equivalent damping ratio empirical curves will be discussed in the following section.

6. Discussion

Centrifuge testing is an effective method to replicate the real loading conditions, stresses and strains, which soil encounters in reality, in small-scaled physical models. As the behaviour of soil is stress and strain dependent, the results obtained from centrifuge tests may more closely reflect the truth in the field than those from 1g model tests.

Although some dynamic properties of saturated sand are improved by fibres, the contribution to liquefaction resistance in this study is not as significant as those mentioned by Maheshwari et al. [19] based on 1g shaking table tests. The maximum excess pore pressure was not apparently reduced when mixing the sand with fibres. One possible explanation is that the confining stresses in those 1g shaking table tests were much less than the prototype. The thickness of the composite deposit in those tests was only 0.6m. Under such a low confining stress, the deposit was more prone to dilate when reinforced by fibres [10]. In the fibre-reinforced deposit of this study, transient dilation was also observed at the shallowest depth according to the occurrence of spikes in the excess pore pressures (Fig. 6) and the stiffening trend in the derived stress strain relationships (Fig. 9). However, soil within the shallowest depths (0~0.6m) accounts for only a small portion of the deposit. Therefore, the overall influence of fibres on reducing excess pore pressures is not significant.

Another possible explanation for less influences of fibres on excess pore pressures may be the difference in input motions. The 1g tests conducted by Maheshwari et al.

[19] were subjected to more intense excitations (sinusoidal) in a rigid box, so the acceleration experienced in the soil of upper layers may not be propagated from the underneath layer but directly exerted by the side walls of the box. Therefore, the entire depth of those models may be excited by the same motion as the base. In centrifuge tests, the excitation at the model bottom is a scaled version of a real earthquake and the deposit depth is more than 10m in prototype. The excitations in the soil at each depth depend on the accelerations propagated to this elevation, which is in line with the circumstance during real earthquakes. The presence of fibres in the sand matrix was better at propagating accelerations (Fig. 5), so more excitation was imparted to the upper layer of the fibre-reinforced model than that of the clean sand. Consequently, higher excess pore pressures tended to be generated in the fibre-reinforced sand. The prolonged time for reaching the maximum value in fibre reinforced sand at the deepest elevation is in line with the observation in shaking table tests. This may be because the excitations between the two models were not hugely different when accelerations were not significantly changed during propagation.

The very limited contribution of fibres to reducing ground settlements, which disagrees with the outcomes from 1g shaking table tests, may also be due to the difference in the propagated accelerations between the fibre-reinforced sand and the clean sand mentioned above. The ground surface settlement is the sum of the settlements of sub-layers within the deposit with free field geostatic condition. Analysing sub-layers independently, those in fibre-reinforced deposits were subjected to stronger motions (with a larger amplitude and more loading cycles). The settlement of sand deposit increases with the cyclic stress ratios and the number of shear excitation cycles [42, 43]. Therefore, the clean sand could have tended to settle more if it had been subjected to the motions experienced by the fibre-reinforced sand. The very similar ground settlement indicates the fact that the fibres may have been beneficial in reducing the ground settlement if the loading condition is the same.

Moreover, the high aspect ratio (the height to the length) of the rigid box results in the 1g shaking table tests results in very complicated stress field, which is different from that in the free field. The reliability of results from those tests is still unclear [44].

The contribution of fibres to shear modulus is more evident when the shear strain increases to a certain level. This is because higher shear strains result in greater mobilisation of fibre tensile strength. This was also observed in monotonic tests in the literature, e.g. the work of Michalowski and Čermák[9] and Diambra et al.[28].

As to the damping ratios, the centrifuge data of the fibre-reinforced sand are generally larger than those of the clean sand at small strains and the differences become less when shear strains increase. The empirical curves agree reasonably with centrifuge data at large strains. However, the indications from the empirical curve are opposite to those from the centrifuge data (Fig. 11(b)). This contradiction may be caused by that the fibre-reinforced sand potentially obtains a certain amount of extra damping ratios at very small shear strains while the empirical equations based on the database of clean sands are not able to describe this. Further work on this is required in the future.

7. Conclusion

Dynamic centrifuge tests were carried out based on a free field condition to investigate the dynamic behaviour of saturated sand. The dry pluviation technique was introduced to prepare the fibre-reinforced sand for centrifuge tests. The effects of fibres on acceleration propagation, excess pore pressure generation and ground surface settlements have been obtained from the comparison of measurements between the clean sand and the fibre-reinforced sand. The influences of fibres on the shear moduli and the equivalent damping ratios are analysed. It is found that:

(1) Fibres have some beneficial effects on propagating accelerations within the deposit which may be the result of their contribution to preventing the collapse of the sand matrix during excitations.

(2) Excess pore pressures and ground settlements are not apparently affected by the presence of fibres in the free field. This may be explained by the different excitation conditions within deposit between the clean sand and the fibre-reinforced sand caused by acceleration propagation. If the same loading conditions are encountered in both types of soil as those in element tests, excess pore pressures and ground settlements may be reduced by the presence of fibres.

(3) Fibres may have the capability to reduce the excess pore pressure generation and ground settlement if the excitations were consistent with that of the clean sand. This was always controlled in laboratory tests, but it is not real in the field. Therefore, the effectiveness of fibre-reinforcement to mitigate liquefaction may be less than suggested by previous research.

(4) The influences of fibres on increasing shear moduli were verified in centrifuge tests and they were more apparent under lower confining stresses and at larger shear strains.

(5) The fibres increased equivalent damping ratios at small shear strains, but this effect becomes less when shear strains increase to a certain level.

This study is based on the specific fibre, soil and loading conditions. More relevant tests should be carried out with other types of fibres, soils and loading conditions to provide more general behaviour of fibre-reinforced sand under dynamic loadings.

Acknowledgements

This study was financially supported by the joint fund of the China Scholarship Council and the University of Dundee. Loksand™ was kindly provided by Drake Extrusion Ltd (UK). The first author would also like to thank the Changjiang River Scientific Research Institute of Changjiang Water Resources Commission for providing software for editing the manuscript at the final stage.

References

[1] K. Ishihara, Liquefaction and flow failure during earthquakes, Géotechnique, 43 (1993) 351-415.

[2] A.J. Brennan, Vertical drains as a countermeasure to earthquake-induced liquefaction, PhD Thesis (2004), University of Cambridge, Cambridge, UK.

[3] D.H. Gray, H. Ohashi, Mechanics of fiber reinforcement in sand, Journal of Geotechnical Engineering, 109 (1983) 335-353.

[4] E. Ibraim, S. Fourmont, Behaviour of Sand Reinforced with Fibres, in: H. Ling, L. Callisto, D. Leshchinsky, J. Koseki (Eds.) Soil Stress-Strain Behavior: Measurement, Modeling and Analysis, Springer, Netherlands, 2007, pp. 807-818.

[5] D.H. Gray, T. Al-Refeai, Behavior of Fabric-Versus Fiber-Reinforced Sand, Journal of Geotechnical Engineering, 112 (1986) 804-820.

[6] M.H. Maher, D.H. Gray, Static response of sands reinforced with randomly distributed fibers, Journal of Geotechnical Engineering, 116 (1990) 1661-1677.

[7] T.O. Al-Refeai, Behavior of granular soils reinforced with discrete randomly oriented inclusions, Geotextiles and Geomembranes, 10 (1991) 319-333.

[8] G. Ranjan, R.M. Vasan, H.D. Charan, Probabilistic Analysis of Randomly Distributed Fiber-Reinforced Soil, Journal of Geotechnical Engineering, 122 (1996) 419-426.

[9] R.L. Michalowski, J. Čermák, Triaxial compression of sand reinforced with fibers, Journal of Geotechnical and Geoenvironmental Engineering, 129 (2003) 125-136.

[10] E. Ibraim, A. Diambra, D. Muir Wood, A.R. Russell, Static liquefaction of fibre reinforced sand under monotonic loading, Geotextiles and Geomembranes, 28 (2010) 374-385.

[11] J. Liu, G. Wang, T. Kamai, F. Zhang, J. Yang, B. Shi, Static liquefaction behavior of saturated fiber-reinforced sand in undrained ring-shear tests, Geotextiles and Geomembranes, 29 (2011) 462-471.

[12] M.H. Maher, R.D. Woods, Dynamic Response of Sand Reinforced with Randomly Distributed Fibers, Journal of Geotechnical Engineering, 116 (1990) 1116-1131.

[13] H. Li, K. Senetakis, Modulus Reduction and Damping Increase of Two Sands Reinforced with Polypropylene Fibers, Journal of Materials in Civil Engineering, 30 (2018) 1-9.

[14] R. Jamshidi, I. Towhata, H. Ghiassian, A.R. Tabarsa, Experimental evaluation of dynamic deformation characteristics of sheet pile retaining walls with fiber reinforced backfill, Soil Dynamics and Earthquake Engineering, 30 (2010) 438-446.

[15] I. Noorany, M. Uzdavines, Dynamic behavior of saturated sand reinforced with geosynthetic fabrics, Proceedings of Geosynthetics '89 Conference, San Diego, USA, 1989.

[16] R. Noorzad, P. Fardad Amini, Liquefaction resistance of Babolsar sand reinforced with randomly distributed fibers under cyclic loading, Soil Dynamics and Earthquake Engineering, 66 (2014) 281-292.

[17] N.R. Krishnaswamy, N. Thomas Isaac, Liquefaction potential of reinforced sand, Geotextiles and Geomembranes, 13 (1994) 23-41.

[18] A. Boominathan, S. Hari, Liquefaction strength of fly ash reinforced with randomly distributed fibers, Soil Dynamics and Earthquake Engineering, 22 (2002) 1027-1033.

[19] B. Maheshwari, H. Singh, S. Saran, Effects of reinforcement on liquefaction resistance of solani sand, Journal of Geotechnical and Geoenvironmental Engineering, 138 (2012) 831-840.

[20] A.J. Brennan, J.A. Knappett, D. Bertalot, M. Loli, I. Anastasopoulos, M.J. Brown, Dynamic centrifuge modelling facilities at the University of Dundee and their application to studying seismic case histories, Physical Modelling in Geotechnics - Proceedings of the 8th International Conference on Physical Modelling in Geotechnics 2014, Perth, Australia, 2014.

[21] A.J. Brennan, S.P.G. Madabhushi, N.E. Houghton, Comparing laminar and equivalent shear beam (ESB) containers for dynamic centrifuge modelling, Physical Modelling in Geotechnics-ICPMG'06, Hong Kong, 2006.

[22] P. Coelho, S.K. Haigh, S.G. Madabhushi, Boundary effects in dynamic centrifuge modelling of liquefaction in sand deposits, Proceedings of the 16th ASCE engineering mechanics conference, University of Washington, Seattle, USA, 2003.

[23] D. Bertalot, Seismic behaviour of shallow foundations on layered liquefiable soils, PhD Thesis (2013), University of Dundee, Dundee, UK.

[24] D.P. Stewart, Y.R. Chen, B.L. Kutter, Experience with the use of methylcellulose as a viscous pore fluid in centrifuge models, Geotechnical Testing Journal, 21 (1998) 365-369.

[25] D. Muir Wood, Geotechnical Modelling, CRC Press, Boca Raton, 2004.

[26] A. Tabaroei, S. Abrishami, E.S. Hosseininia, Comparison between Two Different Pluviation Setups of Sand Specimens, Journal of Materials in Civil Engineering, 29 (2017) 1-11.

[27] K. Wang, Evaluation of Fibre-reinforcement as A Mitigation Method against Earthquake Induced Liquefaction Hazards by Centrifuge Modelling, PhD Thesis (2018), University of Dundee, Dundee, UK.

[28] A. Diambra, E. Ibraim, D. Muir Wood, A.R. Russell, Fibre reinforced sands: Experiments and modelling, Geotextiles and Geomembranes, 28 (2010) 238-250.

[29] K. Ueno, Methods for preparation of sand samples, Centrifuge 98: Proceedings of the International Conference Centrifuge 98, Tokyo, Japan, 1998.

[30] K. Wang, A.J. Brennan, Centrifuge modelling of saturated fibre-reinforced sand, Physical Modelling in Geotechnics - Proceedings of the 8th International Conference on Physical Modelling in Geotechnics 2014, Perth, Australia, 2014.

[31] H.B. Seed, I.M. Idriss, I. Arango, Evaluation of Liquefaction Potential Using Field Performance Data, Journal of Geotechnical Engineering, 109 (1983) 458-482.

[32] M. Omarov, Liquefaction potential and post-liquefaction settlement of saturated clean sands; and effect of geofiber reinforcement, MSc Thesis (2010), University of Alaska Fairbanks, Fairbanks, Alaska, USA.

[33] M. Zeghal, A.W. Elgamal, X. Zeng, K. Arulmoli, Mechanism of liquefaction response in sand-silt dynamic centrifuge tests, Soil Dynamics and Earthquake Engineering, 18 (1999) 71-85.

[34] A.J. Brennan, N.I. Thusyanthan, S.P.G. Madabhushi, Evaluation of shear modulus and damping in dynamic centrifuge tests, Journal of Geotechnical and Geoenvironmental Engineering, 131 (2005) 1488-1497.

[35] E. Apostolou, A.J. Brennan, J. Wehr, Liquefaction characteristics of coarse silt-graded A50 silica flour, 1st International Conference on Natural Hazards and Infrastructure: Protection, Design, Rehabilitation., Chania, Greece, 2016.

[36] B.O. Hardin, V.P. Drnevich, Shear Modulus and Damping in Soils, Journal of the Soil Mechanics and Foundations Division, 98 (1972) 667-692.

[37] M.A. Sherif, I. Ishibashi, Dynamic shear moduli for dry sands, Journal of the Geotechnical Engineering Division, 102 (1976) 1171-1184.

[38] I. Ishibashi, X. Zhang, Unified dynamic shear moduli and damping ratios of sand and clay, Soils and Foundations, 33 (1993) 182-191.

[39] K.V. Talaganov, Stress-strain transformations and liquefaction of sands, Soil Dynamics and Earthquake Engineering, 15 (1996) 411-418.

[40] M.H.T. Rayhani, M.H. El Naggar, Seismic response of sands in centrifuge tests, Canadian Geotechnical Journal, 45 (2008) 470-483.

[41] R. Conti, G.M.B. Viggiani, Evaluation of Soil Dynamic Properties in Centrifuge Tests, Journal of Geotechnical and Geoenvironmental Engineering, 138 (2012) 850-859.

[42] K. Tokimatsu, H. Seed, Evaluation of Settlements in Sands Due to Earthquake Shaking, Journal of Geotechnical Engineering, 113 (1987) 861-878.

[43] T.S. Ueng, C.W. Wu, H.W. Cheng, C.H. Chen, Settlements of saturated clean sand deposits in shaking table tests, Soil Dynamics and Earthquake Engineering, 30 (2010) 50-60.

[44] A. Sawicki, M. Kulczykowski, Discussion of "Effects of Reinforcement on Liquefaction Resistance of Solani Sand" by B. K. Maheshwari, H. P. Singh, and Swami Saran, Journal of Geotechnical and Geoenvironmental Engineering, 139 (2013) 1633-1634.

Figures

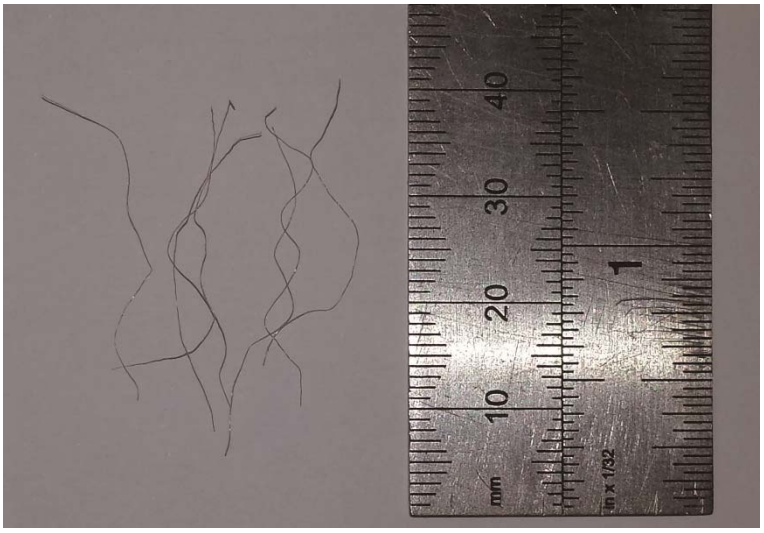

Fig. 1. Loksand^{TM} polypropylene fibres

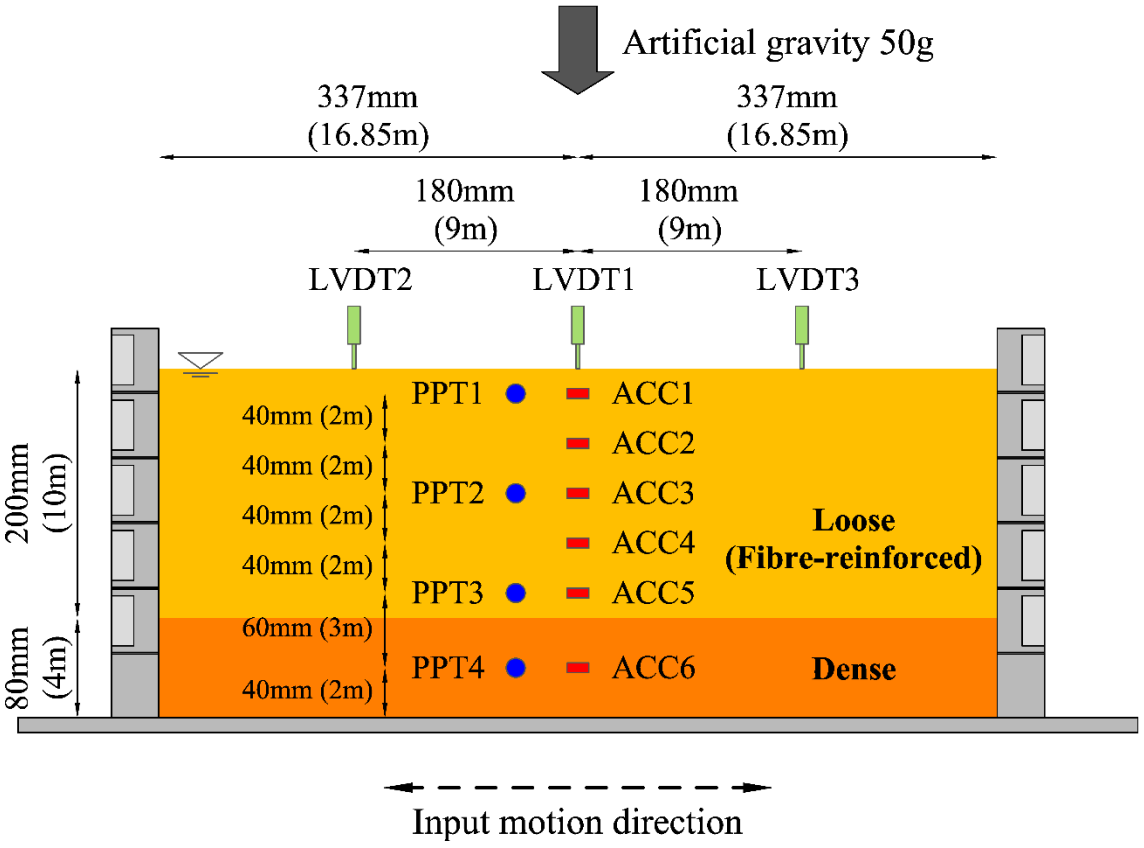

Fig. 2. Model layout and instrument distribution

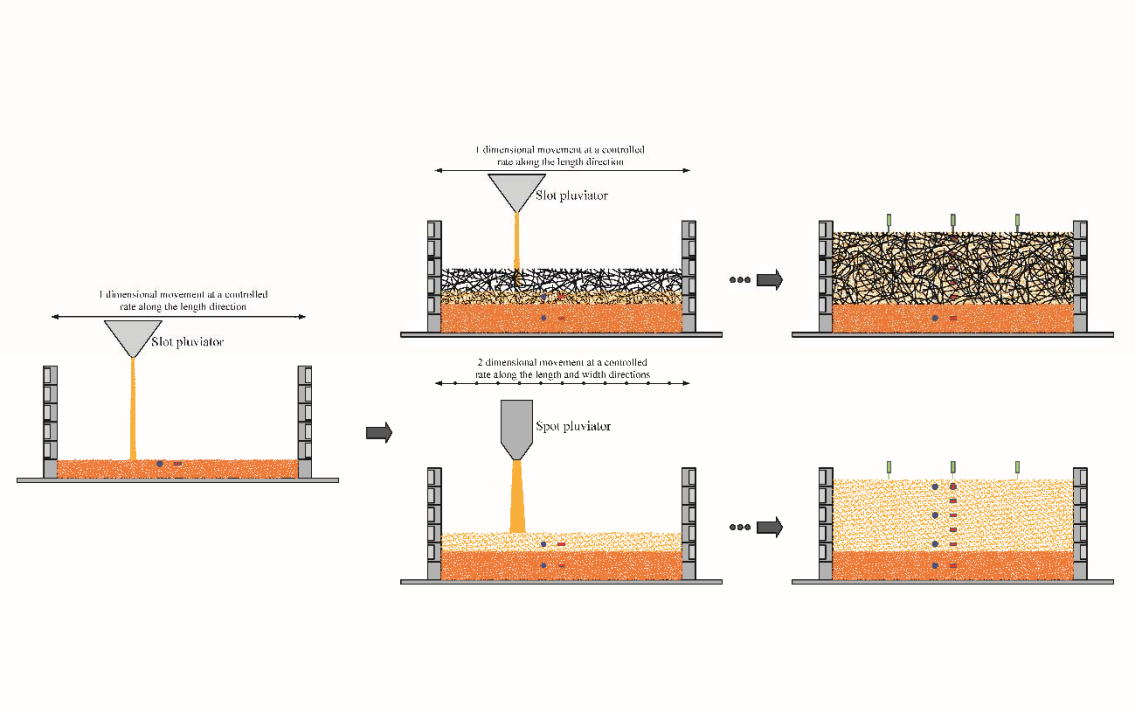

Fig. 3. Dry pluviation procedures

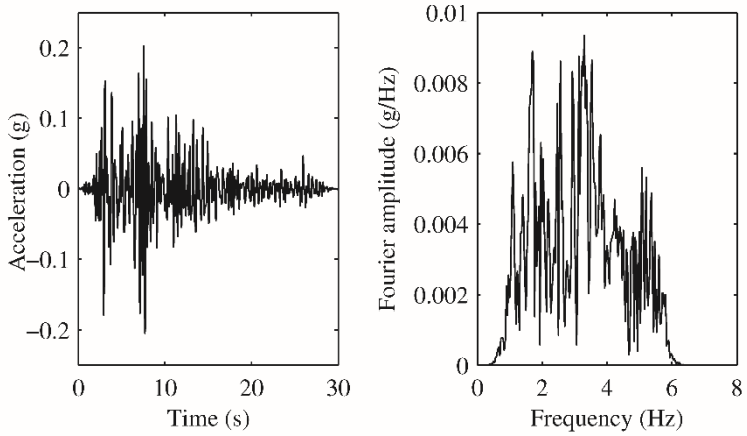

Fig. 4. Selected Kocaeli earthquake motion

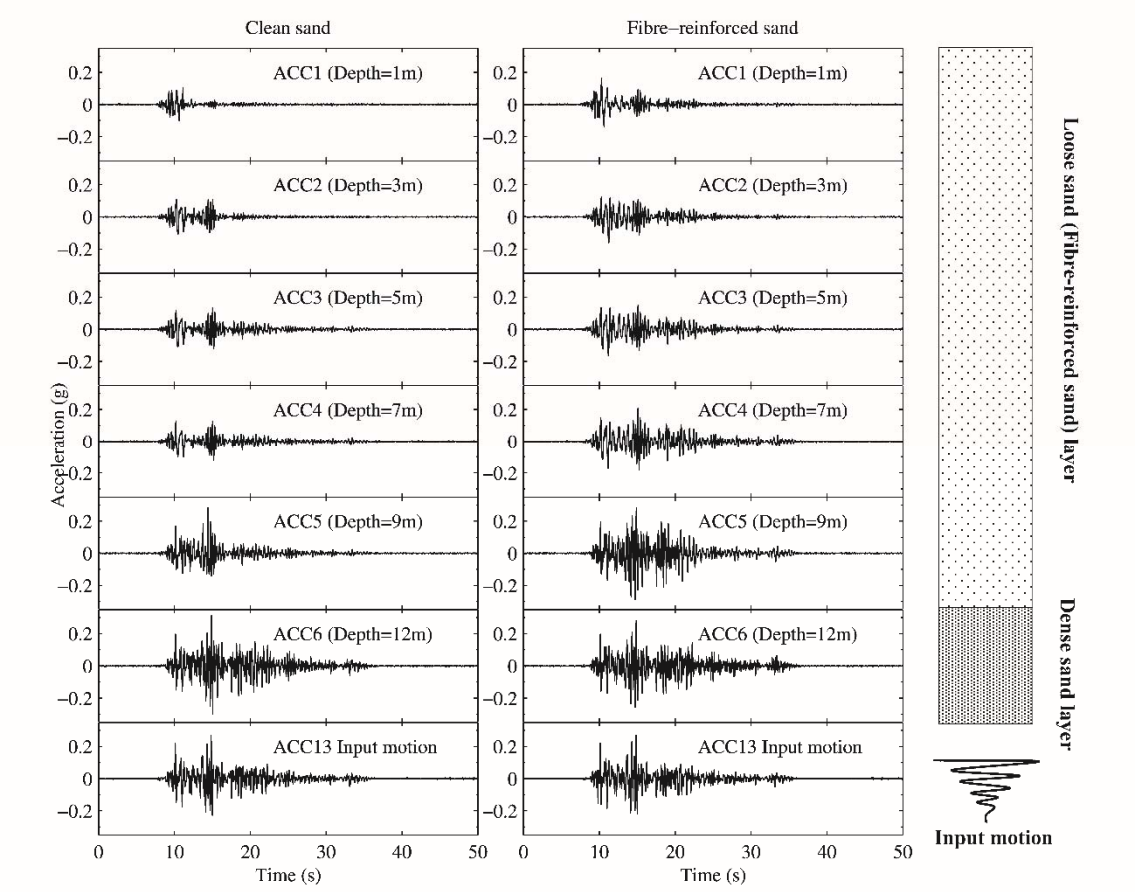

Fig. 5. Acceleration time histories at various depths

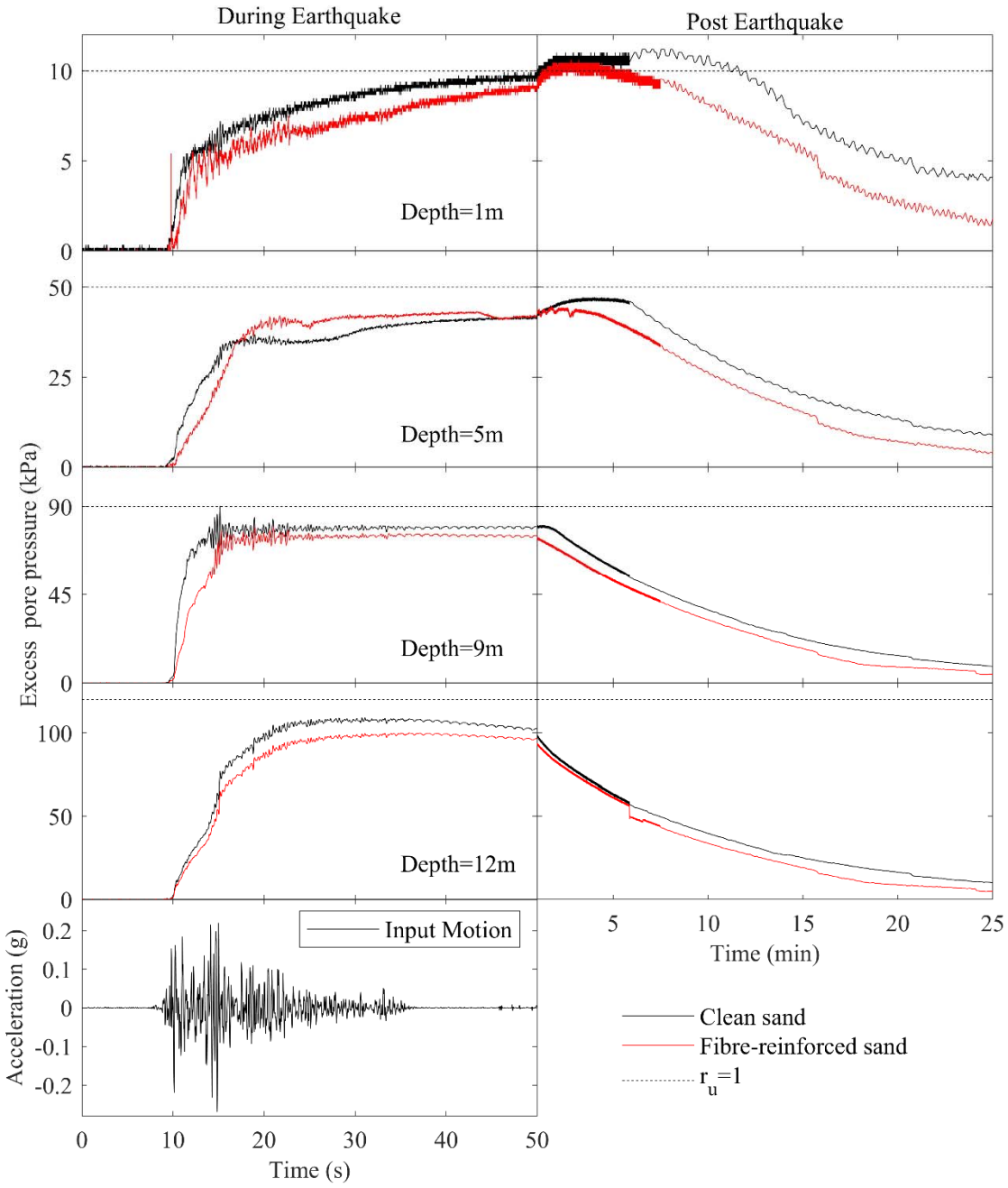

Fig. 6. Excess pore pressure generation and dissipation time histories

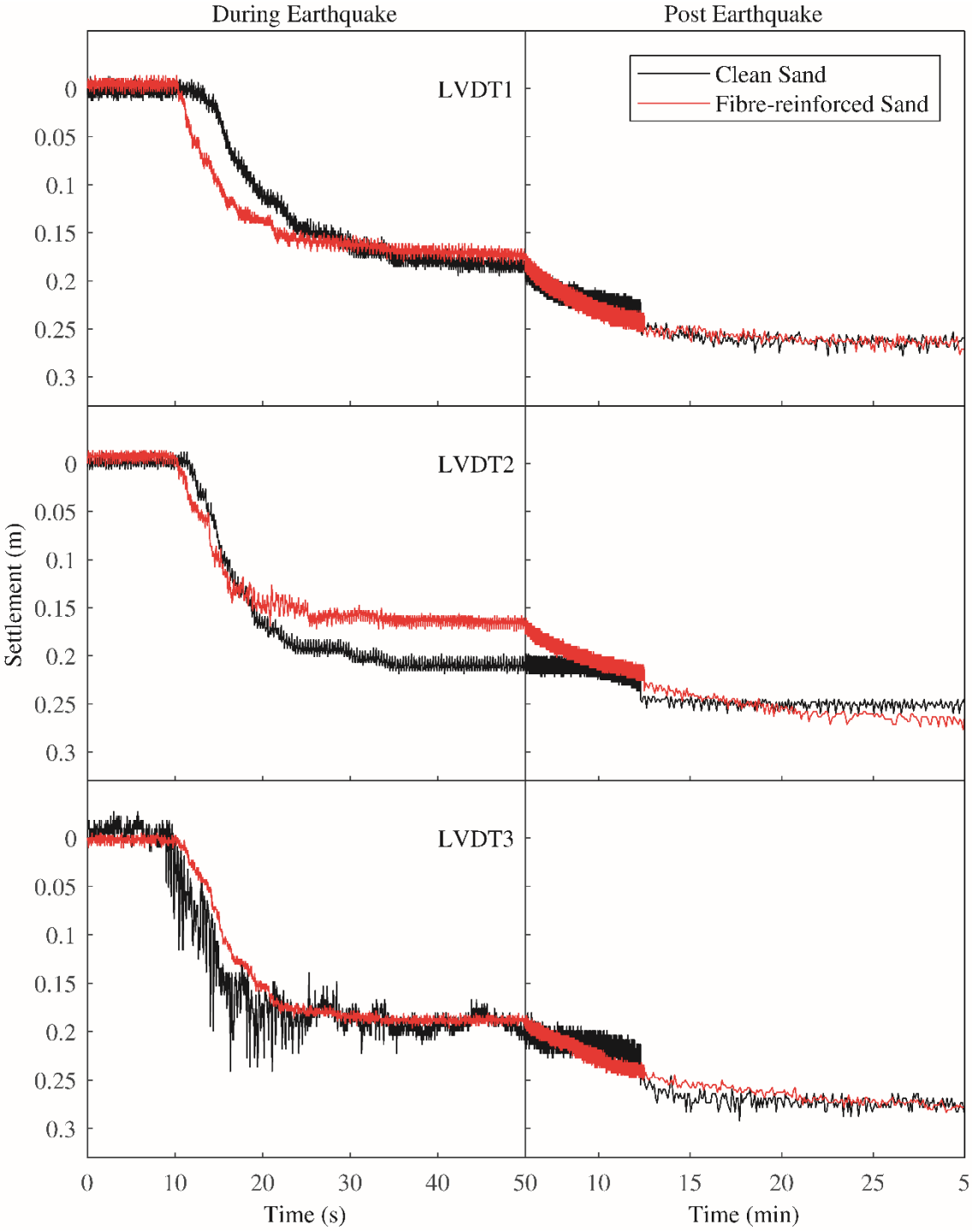

Fig.7. Ground surface settlement time histories

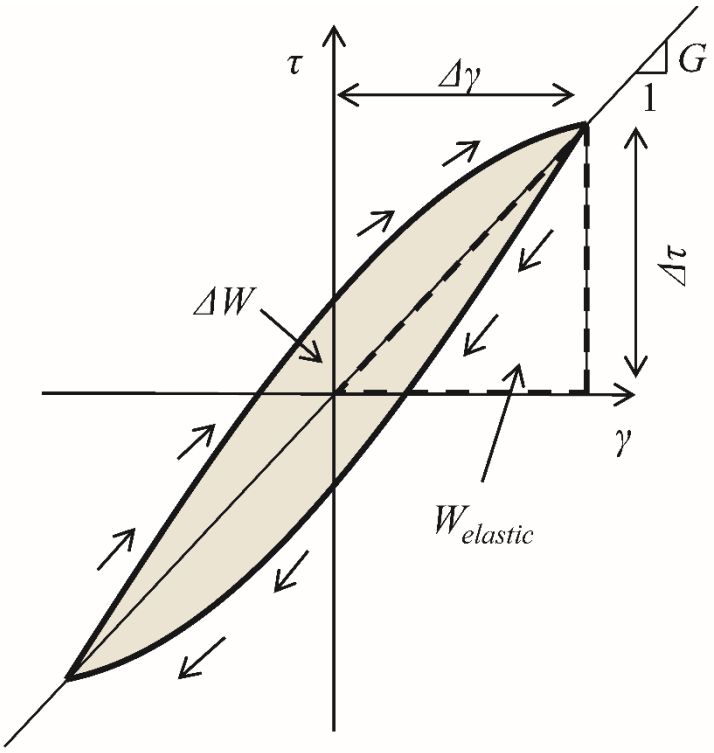

Fig. 8 Schematic demonstration of a shear stress-strain relationship

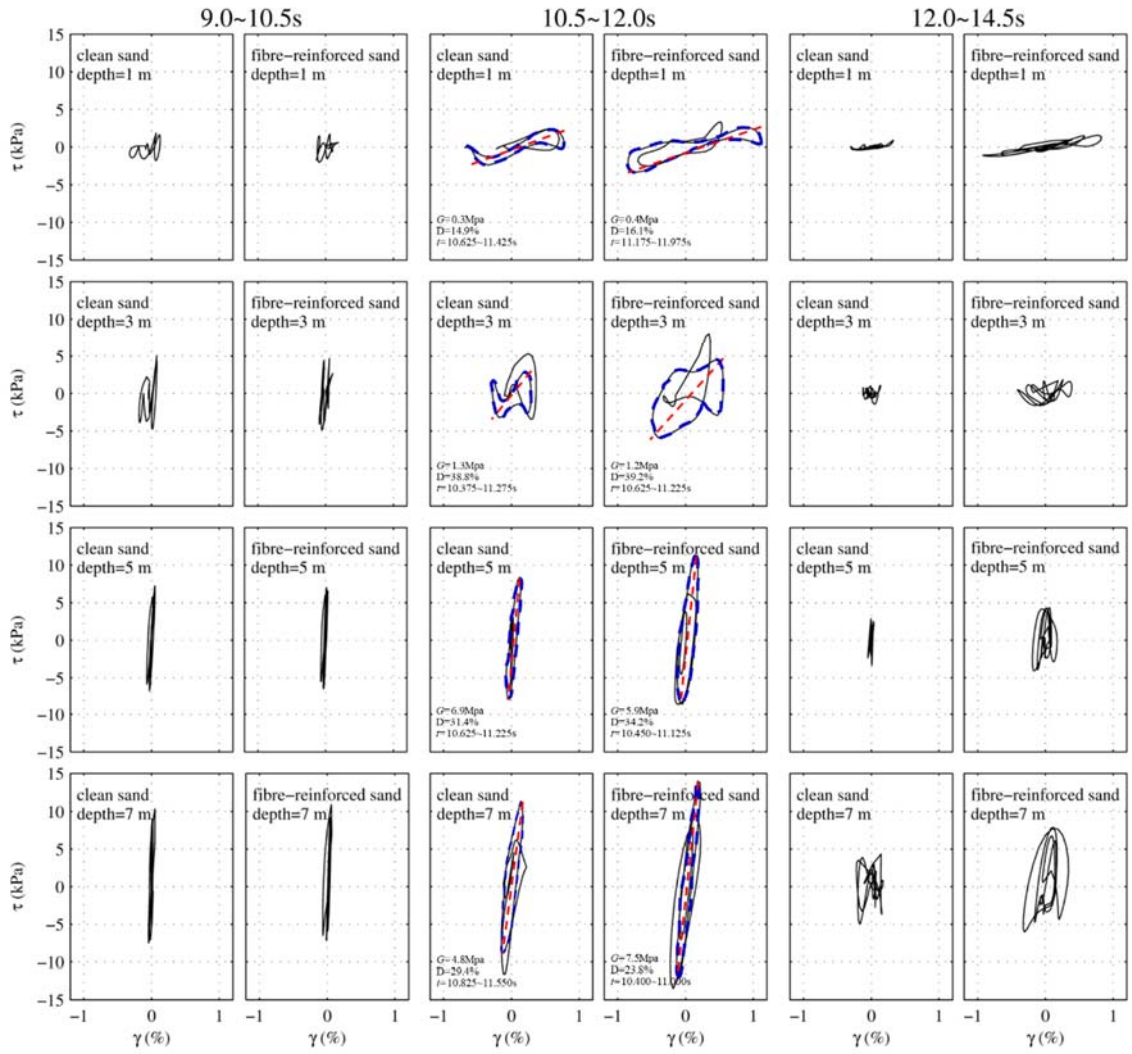

Fig. 9 Shear stress strain time histories at various depths

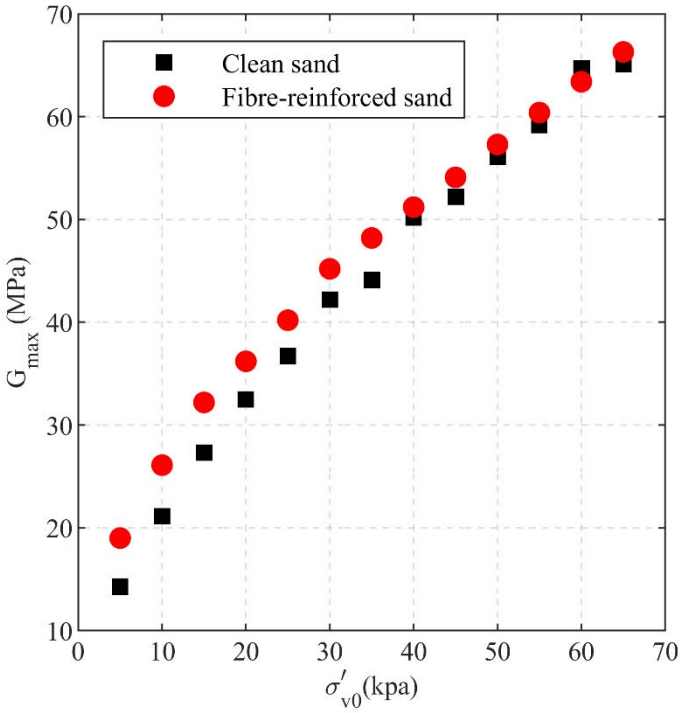

Fig. 10 Variations in G_{max} with effective vertical confining stresses

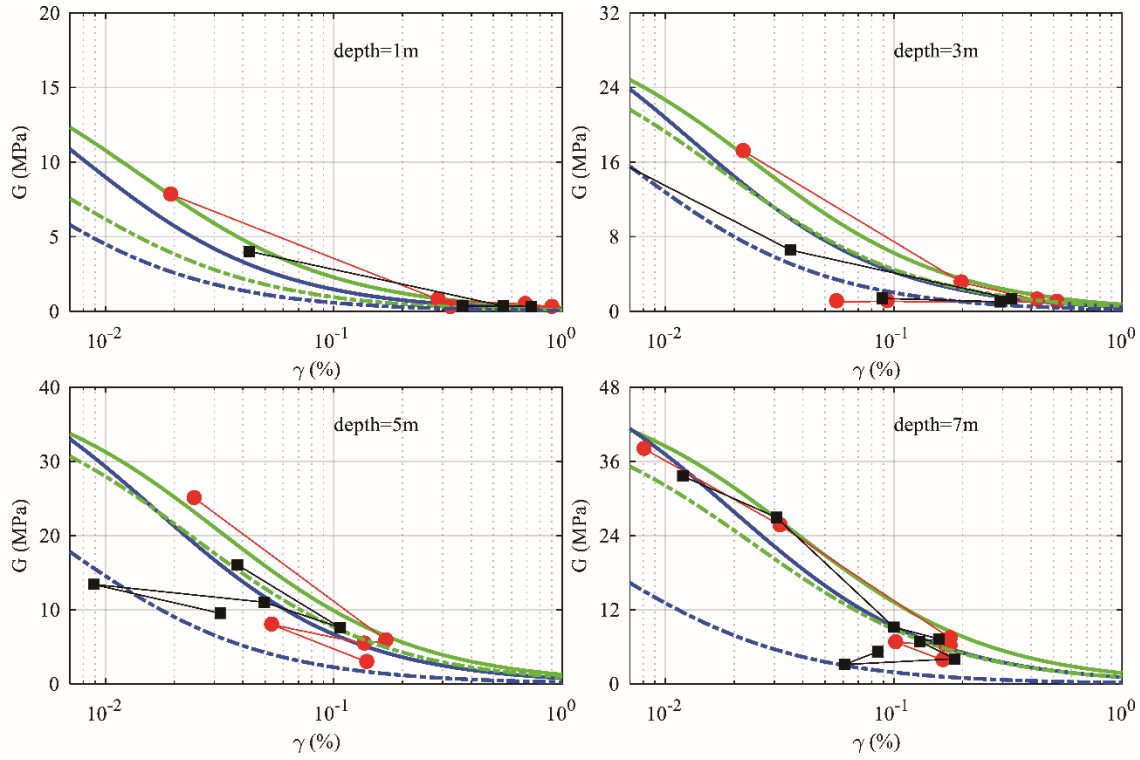
depth=1m
depth=3m
depth=5m
depth=7m
G (MPa)
γ (%)

(a)

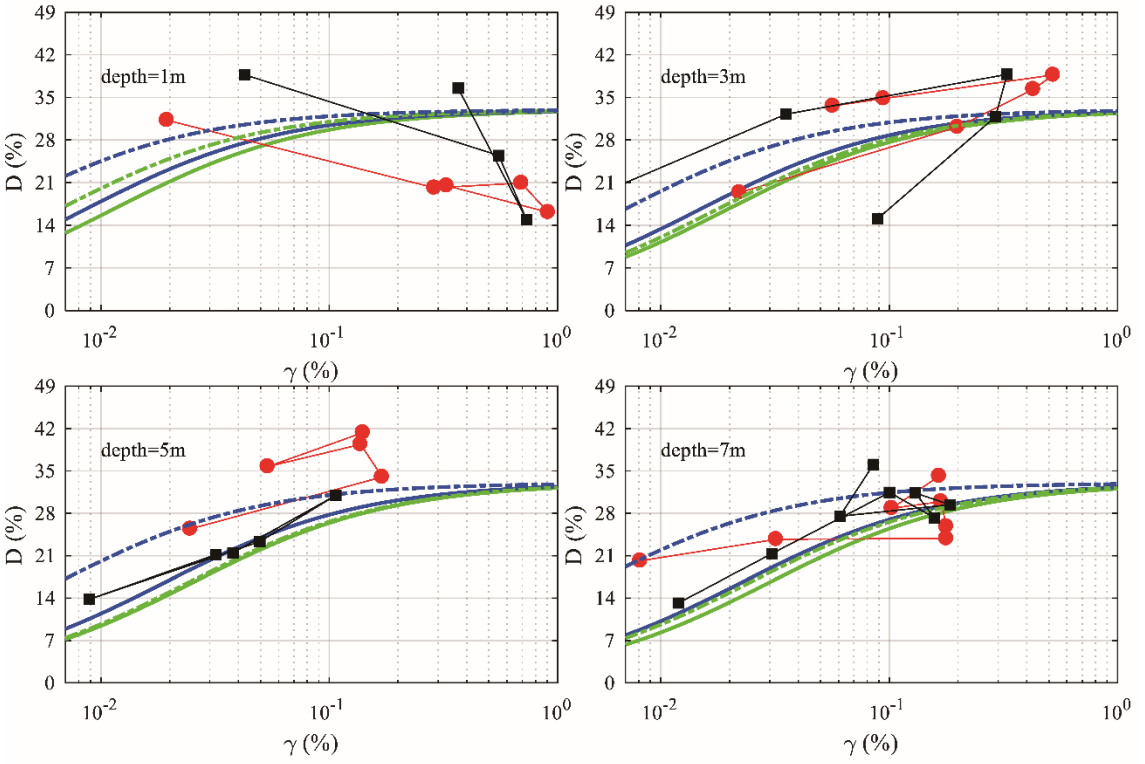
depth=1m
depth=3m
depth=5m
depth=7m
D (%)
γ (%)

(b)

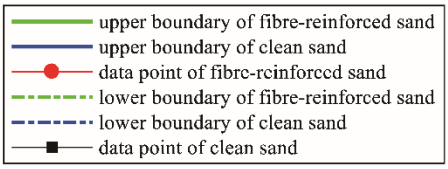
upper boundary of fibre-reinforced sand
upper boundary of clean sand
data point of fibre-reinforced sand
lower boundary of fibre-reinforced sand
lower boundary of clean sand
data point of clean sand

Fig. 11 G-γ and D-γ relationships at various depths

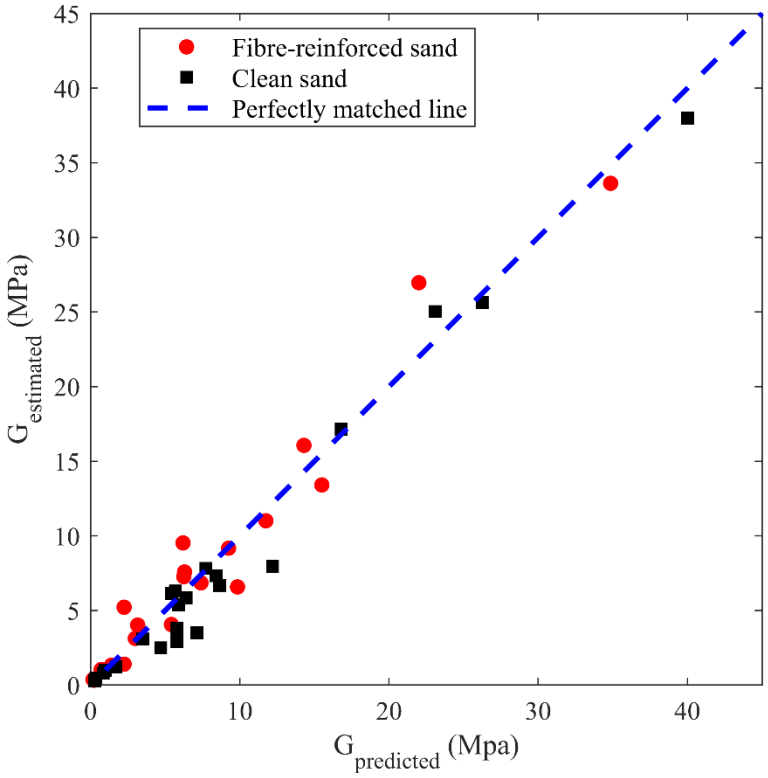

Fig. 12 Comparison between estimated and predicted shear moduli

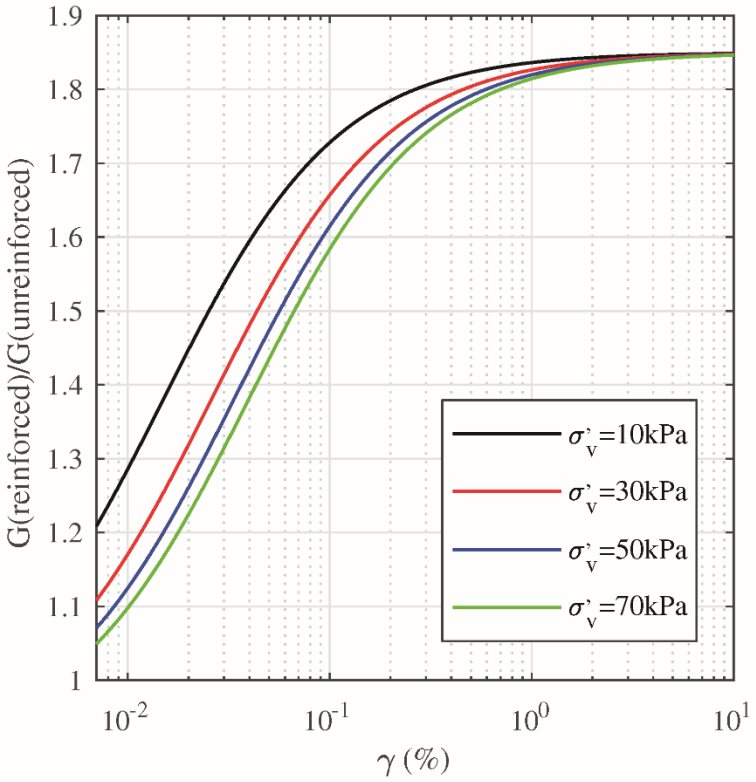

Fig. 13 Influences of γ and σ_v' on the contribution of fibres to shear modulus

Tables

Table 1 Physical properties of HST 95 Congleton sand

Properties	Values
Effective size	D_{10}=0.08mm
Mean size	D_{50}=0.17mm
Coefficient of uniformity	C_u=2.25
Coefficient of curvature	C_c=1.36
Specific gravity	G_s=2.63
Maximum void ratio	e_{max}=0.795
Minimum void ratio	e_{min}=0.463

Table 2 Physical properties of Loksand^{TM}

Properties	Values
Nominal length	35mm
Nominal diameter	0.088mm
Specific gravity	0.91
Tensile strength	200MPa
Crimp level	0.6-1.2crimps/cm